Liquid Crystals
Publication details, including instructions for authors and subscription information:
http://www.informaworld.com/smpp/title~content=t713926090

Mesomorphism of a banana mesogen: influence of a fluoro substituent in the central core

Nandiraju V. S. Rao[a]; Rajdeep Deb[a]; Manoj Kr Paul[a]; Tuluri Francis[b]
[a] Department of Chemistry, Assam University, Silchar, India [b] Department of Technology, Jackson State University, Jackson, MS, USA

To cite this Article Rao, Nandiraju V. S. , Deb, Rajdeep , Paul, Manoj Kr and Francis, Tuluri(2009) 'Mesomorphism of a banana mesogen: influence of a fluoro substituent in the central core', Liquid Crystals, 36: 9, 977 — 987
To link to this Article: DOI: 10.1080/02678290903165979
URL: http://dx.doi.org/10.1080/02678290903165979

Liquid Crystals,
Vol. 36, No. 9, September 2009, 977–987

Taylor & Francis
Taylor & Francis Group

Mesomorphism of a banana mesogen: influence of a fluoro substituent in the central core

Nandiraju V.S. Rao[a]*, Rajdeep Deb[a], Manoj Kr Paul[a] and Tuluri Francis[b]

[a]*Department of Chemistry, Assam University, Silchar 788011, India;* [b]*Department of Technology, Jackson State University, Jackson, MS 39217, USA*

The results of experiments with stable five-ring banana-shaped molecules consisting of laterally 4-fluoro substituted 1,3-phenylene ring as the central unit in Bis-[4-(4′-n-alkyloxybenzoyloxy)salicylidene]-phenylene-4-fluoro-1,3-diamines are presented. These compounds are thermally and hydrolytically stable due to intermolecular or intramolecular hydrogen bonding and exhibit $SmCP_A$ and low-temperature crystalline B_X phases. The phases had been characterised by thermal microscopy and differential scanning calorimetry. A representative example has also been characterised by X-ray diffraction studies and electric field effects. The influence of a lateral fluoro substituent in the central core is clearly demonstrated with the induction of the $SmCP_A$ phase which is absent in the parent compound without the substituent. Further these compounds exhibit a large tilt angle. We also describe a comparison of phase behaviour with similar analogous compounds, taking the position of fluoro substitution, changes in the linking groups and the direction of the linking groups into consideration.

Keywords: Banana shaped mesogens; Fluoro compounds; $SmCP_A$ phases; Spontaneous polarization

1. Introduction

Banana-shaped mesogenic materials represent a fruitful and stimulating field of research, which are interesting both from an academic and an application-based point of view (*1–7*). The brief history of this research area has seen a number of interesting topics; some breathed new life to research and brought new expectations while some of them are open to investigation. The liquid crystalline phase behaviour of bent or banana-shaped compounds is dependent upon several factors, namely the size of the molecule and the number of aromatic rings, the position as well as the magnitude of the bent angle, the size, number, position and nature of the substituents, the nature and direction of linkage groups and the length and nature of the terminal alkyl chains. In general, any minor change in these structural elements leads to drastic changes in the phase behaviour. One of the important aspects is the nature and size of the substituent in the central core, which largely influences the mesophase behaviour (*8*). Several research groups studied the influence of the lateral substituents on the mesophase behaviour either in the central core or the outer rings (*7–9*). However, the introduction of a small substituent into the central 1,3-phenylene ring leads to the possibility of synthesising new mesogens with novel banana phases (*7*, *10*). Moreover, it was found that mesophase behaviour is much more strongly influenced by substituents at the central core than by these at the outer ring (*11*).

The influence of fluorine substitution depending upon its position in banana-shaped molecules revealed several interesting factors. The two important characteristics of a fluorine atom (*12*) are its size and its electro-negativity. The size of the fluorine atom (1.47 Å) which is slightly larger than the hydrogen atom (1.2 Å) contributes towards the steric intermolecular interactions. Further the electro-negativity of the fluorine atom exhibit a strong influence on the intermolecular interactions reflecting in the local dipole moments, electron density of the phenyl ring system, which in turn influences the π–π stacking of phenyl rings, π–H–C electrostatic interactions between phenyl rings, polarisation and polarisability of the entire molecular conjugated system [12].

Moreover, the molecular conformation which is dependent upon linking groups being influenced by the steric, stereo-electronic and polar effect reflects in the molecular conformation and minimisation of rotational energy of these molecules. In fact, the bulky and electronegative 4-chloro substitution in bent shaped molecules influenced the mesomorphism not only by a decrease in the clearing temperatures and mesomorphic range but also suppressed the B3 and B4 phases (*7b*). Similarly the 4-cyano substitution leads to the appearance of calamitic phases (smectic A (SmA) and smectic C (SmC)) with suppression of B3 and B4 phases and enhanced B2 phase (*7c*). Hence, the substitution with a highly polar substituent, particularly F on the central 1,3-phenylene core, is of special interest owing to its distinct influence on the properties of bent core mesogens.

The majority of banana-shaped liquid crystals usually comprise 1,3-phenylene-bis-benzoates incorporating at least one Schiff base unit (*2*, *7*, *13*) because of the ease of synthesis and promesogenic-promoting

*Corresponding author. Email: drnvsrao@gmail.com

ISSN 0267-8292 print/ISSN 1366-5855 online

DOI: 10.1080/02678290903165979
http://www.informaworld.com

character of this particular linkage. However, the important limitations of the compounds possessing the imine linkage are thermal, hydrolytic and photochemical stability. These limitations can be addressed with an ortho hydroxyl group to imine linkage which stabilises the compound. Hence, as part of our work on substituted banana-shaped mesogens with an ester–imine combination, we report a new class of banana-shaped mesogens with a fluoro substituent on the central core and a lateral hydroxyl group ortho to imine linkage which participates in intramolecular or intermolecular H-bonding to stabilise the imine linkage and thereby promoting non-covalent self-assembly with a hope for new findings about the influence of highly polar substituents especially via new combination of linking group and lateral substituents.

2. Experimental details

2.1 General

All of the chemicals, namely 4-hydroxy-ethylbenzoate, 1-bromo-n-alkanes, 1-fluoro-2,4-dintrobenzene, 2,4-dihydroxybenzaldehyde were procured and used as received from either Tokyo Kasei Kogyo Co. Ltd., Avocado Chemicals or E-Merck. Silica gel (60–120 mesh, Acme synthetic chemicals) was used for chromatographic separation. Silica gel G [E-Merck] was used for thin layer chromatography (TLC). The solvents and reagents are of AR grade and were distilled and dried before use following standard procedures. TLC was performed on glass slides pre-coated with silica gel. The intermediate compounds were purified by column chromatography using silica gel. All of the compounds were characterised by elemental analysis, infrared (IR) spectra (Perkin-Elmer L120-000A spectrometer), and by ^{1}H nuclear magnetic resonance (NMR) spectroscopy (JEOL AL 300 FT NMR in $CDCl_3$ solution, chemical shifts are reported in parts per million (δ) relative to tetramethylsilane (TMS) as an internal standard).

The liquid-crystal cells were placed in a computer-controlled heating stage (hot and cold stage HCS302, with STC200 temperature controller configured for HCS302 from INSTEC) and the optical textures inferring the phase sequences were investigated by polarising microscopy (Nikon polarising microscope OPTIPHOT-POL2). The phase transition temperatures and associated enthalpies of transition were determined by differential scanning calorimetry (DSC; Perkin-Elmer DSC Pyris1 system that was calibrated previously using pure indium as a standard). The heating and cooling rates were 5 or 10°C per minute. The electrical switching characteristics of the liquid-crystalline phase were investigated using commercial cells made of indium tin oxide (ITO)-coated glass plates, spaced by 5 μm, with unidirectional pretreated polyimide solution, which enable the homogeneous alignment of the molecules. These transparent cells were filled with the liquid-crystalline samples in the isotropic phase by a capillary action. The electro-optical switching features were observed under the microscope. The X-ray diffraction analyses were carried out using unoriented sample contained in 1 mm diameter quartz capillary tubes and data were collected using a point detector mounted on a Huber four-circle goniometer at Cu K(α) radiation from a Rigaku UltraX-18 rotating anode generator.

2.2 Synthesis and molecular structural characterisation

The synthetic route followed to obtain the compounds of banana-shaped molecules 3-*n*OHF (*n* being the number of carbon atoms in the end aliphatic chain), following the standard procedures (*14*) with minor modifications is presented in Scheme 1. The target compounds, namely the derivatives of substituted 1,3-phenylenes (3-*n*OHF series) were prepared by acid catalyzed condensation of 4-fluro-1,3-phenylenediamine with two equivalents of the respective 4-(4′-n-alkyloxybenzoyloxy)salicylaldehyde (**2-*n***) with a catalytic amount of glacial acetic acid in absolute alcohol. The required 4-(4′-n-alkyloxy benzoyloxy)salicylaldehydes (**2-*n***) were prepared by condensation of 4-n-alkoxybenzoyl chloride with 2,4-dihydroxybenzaldehydes in the presence of a catalytic amount of triethylamine in dichloromethane. The crude materials obtained were purified by column chromatography and recrystallised from a suitable solvent. The molecular structures of all of the compounds and intermediates were confirmed by spectroscopic methods of analyses and the results are presented in Section 2.3.

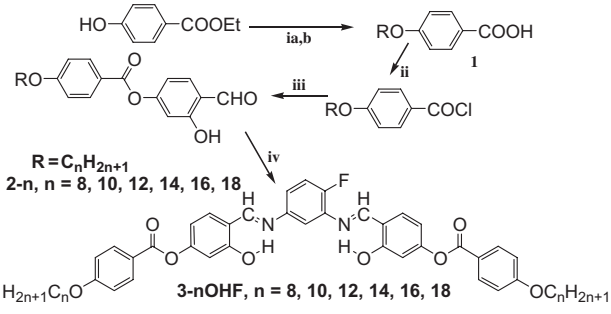

Scheme 1. **ia** KOH, EtOH, RBr, Kl, Δ, 24h; **b)** OH^-, H_2O, H^+ **ii)** $SOCl_2$, Δ, 1h **iii)** TEA, 2,4-dihydroxybenzaldehyde,DCM,6h **iv)** 4-fluoro-1,3-phenylendiamine, Abs EtOH, AcOH, Δ, 3h.

2.3 Analytical data

All of the desired compounds were synthesised following the standard procedures (*14*) with minor modifications as presented in Scheme 1. The 4-n-alkoxy benzoic acids were synthesised using Williamson ether synthesis.

2–8: 4-(4′-n-octyloxybenzoyloxy)salicylaldehyde, white solid. Yield 3.49 g (63%), melting point (MP) = 84.9°C. IR ν_{max} (in cm^{-1}): 1680 (ν_{CHO}); 1736 ($\nu_{C=O}$, ester); 3400 (ν_{OH}, H-bonded) cm^{-1}; ^1H NMR ($CDCl_3$, 300 MHz): δ = 11.26 (s, 1H, –OH); 9.89 (s, 1H, –CHO); 8.12 (dd, 2H, *J* = 2.4, 8.9 Hz, ArH); 7.60 (d, 1H, *J* = 8.4 Hz, ArH); 6.99 (dd, 2H, *J* = 2.4, 8.9 Hz, ArH); 6.90 (dd, 1H, *J* = 1.8, 8.5 Hz, ArH); 6.87 (d, 1H, *J* = 2.0 Hz, ArH), 4.05 (t, 2H, *J* = 6.6 Hz), 1.83 (q, 2H, *J* = 6.6 Hz), 1.28–1.58 (m, 10H), 0.89 (t, 3H, *J* = 6.6 Hz).

2–10: 4-(4′-n-decyloxybenzoyloxy)salicylaldehyde, MP = 81.3°C,

2–12: 4-(4′-n-dodecyloxybenzoyloxy)salicylaldehyde, MP = 78.7°C,

2–14: 4-(4′-n-tetradecyloxybenzoyloxy)-salicylaldehyde, MP = 81.9°C

2–16: 4-(4′-n-hexadecyloxybenzoyloxy)salicylaldehyde, MP = 76.7°C

2–18: 4-(4′-n-octadecyloxybenzoyloxy) salicylaldehyde, MP = 82.7°C

3–80HF: N,N′-bis[4-(4-*n*-octyloxybenzoyloxy)salicylidene]-phenylene-4-fluoro-1,3-diamine. An ethanolic solution (20 ml) of 4-(4′-n-octyloxybenzoyloxy)salicylaldehyde (0.92 g, 2.5 mmol) was added to an ethanolic solution of 4-fluoro-1,3-phenylene diamine (0.15 g, 1.25 mmol). The mixture was refluxed with a few drops of glacial acetic acid as catalyst for 3 hours to yield the Schiff's base N,N′-bis[4-(4-*n*-octyloxybenzoyloxy)salicylidene]-phenylene-4-fluoro-1,3-diamine The precipitate was collected by filtration from the hot solution and recrystallised several times from absolute ethanol to give a pure compound. Yield 0.70 g (68%). IR ν_{max} (in cm^{-1}); 1632 ($\nu_{C=N}$, imine); 1734 ($\nu_{C=O}$, ester); 3444 (ν_{OH}, H-bonded); ^1H NMR ($CDCl_3$, 300MHz): δ = 13.24 (bs, 2H, –OH); 8.75 and 8.60 (s, 2H, –CH=N); 8.11 (d, 4H, *J* = 8.7 Hz, ArH); 8.08 (d, 2H, *J* = 8.4 Hz, ArH); 7.45 (d, 1H, *J* = 7.6 Hz, ArH); 7.16 (d, 2H, *J* = 8.8 Hz, ArH); 7.10 (d, 1H, *J* = 2.1 Hz, ArH); 6.95 (d, 1H, *J* = 7.6 Hz, ArH); 6.89 (d, 2H, *J* = 2.3 Hz, ArH); 6.85 (d, 4H, *J* = 8.7 Hz, ArH); 4.03 (t, 4H, *J* = 6.4 Hz, –O–**CH_2**); 1.82 (q, 4H, *J* = 6.8 Hz, –CH_2– **CH_2**–); 1.60-1..24 (m, 20H, **–$(CH_2)_5$**–); 0.98 (t, 6H, *J* = 6.8 Hz, –**CH_3**). Elemental analysis calculated for $C_{50}H_{55}O_8N_2F$ C = 72.27%; H = 6.67%; N = 3.37%. Found C = 72.80%; H = 6.89%; N = 3.52%.

3–10OHF: N, N′-bis[4-(4-*n*-decyloxybenzoyloxy)-salicylidene]-phenylene-4-fluoro-1,3-diamine. Yield 0.73 g (66%). IR ν_{max} (in cm^{-1}); 1626 ($\nu_{C=N}$, imine); 1738 ($\nu_{C=O}$, ester); 3423 (ν_{OH}, H-bonded); ^1H NMR ($CDCl_3$, 300MHz): δ = 13.26 (bs, 2H, –OH); 8.77 and 8.64 (s, 2H, –CH=N); 8.13 (d, 4H, *J* = 7.8 Hz, ArH); 8.11 (d, 2H, *J* = 8.4 Hz, ArH); 7.46 (d, 1H, *J* = 7.2 Hz, ArH); 7.11 (d, 2H, *J* = 8.4, ArH); 6.98 (d, 1H, *J* = 2.4 Hz, ArH); 6.96 (d, 1H, *J* = 8.4 Hz, ArH); 6.91 (d, 2H, *J* = 2.8 Hz, ArH); 6.82 (d, 4H, *J* = 8.4 Hz, ArH); 4.04 (t, 4H, *J* = 6.0 Hz, –O–**CH_2**); 1.82 (q, 4H, *J* = 6.6 Hz, –CH_2– **CH_2**–); 1.60–1.28 (m, 28H, **–$(CH_2)_7$**–); 0.88 (t, 6H, *J* = 6.6 Hz, –**CH_3**). Elemental analysis calculated for $C_{54}H_{63}O_8N_2F$ C = 73.11%; H = 7.16%; N = 3.16%. Found C = 73.53%; H = 7.24%; N = 3.21%.

3–12OHF: N, N′-bis[4-(4-*n*-dodecyloxybenzoyloxy)-salicylidene]-phenylene-4-fluoro-1,3-diamine. Yield 0.76 g (61%). IR ν_{max} (in cm^{-1}); 1632 ($\nu_{C=N}$, imine); 1733 ($\nu_{C=O}$, ester); 3422 (ν_{OH}, H-bonded); ^1H NMR ($CDCl_3$, 300MHz): δ = 13.26 (bs, 2H, –OH); 8.77 and 8.65 (s, 2H, –CH=N); 8.14 (d, 4H, *J* = 8.7 Hz, ArH); 8.12 (d, 2H, *J* = 8.2 Hz, ArH); 7.47 (d, 1H, *J* = 8.1 Hz, ArH); 7.45 (d, 2H, *J* = 8.4 Hz, ArH); 7.13 (d, 1H, *J* = 2.1 Hz, ArH); 6.97 (d, 1H, *J* = 8.4 Hz, ArH); 6.94 (d, 2H, *J* = 2.1 Hz, ArH); 6.85 (d, 4H, *J* = 8.4 Hz, ArH); 4.05 (t, 4H, *J* = 6.6 Hz, –O–**CH_2**); 1.82 (q, 4H, *J* = 6.8 Hz, –CH_2– **CH_2**–); 1.55–1.26 (m, 36H, **–$(CH_2)_9$**–); 0.88 (t, 6H, *J* = 6.6 Hz, –**CH_3**). Elemental analysis calculated for $C_{58}H_{71}O_8N_2F$ C = 73.86%; H = 7.59%; N = 2.97%. Found C = 73.26%; H = 7.49%; N = 2.65%.

3–14OHF: N, N′-bis[4-(4-*n*-tetradecyloxybenzoyloxy)salicylidene]-phenylene-4-fluoro-1,3-diamines. Yield 0.85 g (65%). IR ν_{max} (in cm^{-1}); 1626 ($\nu_{C=N}$, imine); 1731 ($\nu_{C=O}$, ester); 3420 (ν_{OH}, H-bonded); ^1H NMR ($CDCl_3$, 300MHz): δ = 13.26 (bs, 2H, –OH); 8.77 and 8.65 (s, 2H, –CH=N); 8.13 (d, 4H, *J* = 8.6 Hz, ArH); 8.11 (d, 2H, *J* = 8.4 Hz, ArH); 7.47 (d, 1H, *J* = 8.5 Hz, ArH); 7.44 (d, 2H, *J* = 8.4 Hz, ArH); 7.11 (d, 1H, *J* = 2.4 Hz, ArH); 6.99 (d, 1H, *J* = 8.8 Hz, ArH); 6.96 (d, 2H, *J* = 2.5 Hz, ArH); 6.85 (d, 4H, *J* = 8.4 Hz, ArH); 4.05 (t, 4H, *J* = 6.4 Hz, –O–**CH_2**); 1.82 (q, 4H, *J* = 6.7 Hz, –CH_2– **CH_2**–); 1.55–1.26 (m, 44H, –**$(CH_2)_{11}$**–); 0.88 (t, 6H, *J* = 6.6 Hz, –**CH_3**). Elemental analysis calculated for $C_{62}H_{79}O_8N_2F$, C = 74.52%; H = 7.97%; N=2.80%. Found C = 74.60%; H = 7.93%; N = 2.91%.

3–16OHF: N, N′-bis[4-(4-*n*-hexadecyloxybenzoyloxy)salicylidene]-phenylene-4-fluoro-1,3-diamines. Yield 0.8g (65%). IR ν_{max} (in cm^{-1}); 1629 ($\nu_{C=N}$, imine); 1733 ($\nu_{C=O}$, ester); 3421 (ν_{OH}, H-bonded); ^1H NMR ($CDCl_3$, 300MHz): δ = 13.29 (bs, 2H, –OH); 8.72 and 8.63 (s, 2H, –CH=N); 8.14 (d, 4H, *J* = 8.2 Hz, ArH); 8.09 (d, 2H, *J* = 8.6 Hz, ArH); 7.45 (d, 1H, *J* = 8.6 Hz, ArH); 7.41 (d, 2H, *J* = 8.3 Hz, ArH); 7.08 (d, 1H, *J* = 2.1 Hz, ArH); 6.98 (d, 1H, *J* = 8.7 Hz, ArH); 6.96 (d, 2H, *J* = 2.3 Hz, ArH); 6.84 (d, 4H, *J* = 8.1 Hz, ArH); 4.08 (t, 4H, *J* = 6.3 Hz, –O–**CH_2**); 1.81 (q, 4H, *J* = 6.6 Hz, –CH_2– **CH_2**–); 1.53–1.25 (m, 52H, **–$(CH_2)_{13}$**); 0.87 (t, 6H,

J = 6.3 Hz, –**CH_3**). Elemental analysis calculated for $C_{66}H_{87}O_8N_2F$ C = 75.11%; H = 8.31%; N = 2.65%. Found C = 75.10%; H = 8.36%; N = 2.66%.

3–18OHF: N, N′-bis[4-(4-*n*-octadecyloxybenzoyloxy)salicylidene]-phenylene-4-fluoro-1,3-diamines. Yield 0.8g (65%). IR ν_{max} (in cm^{-1}); 1630 ($\nu_{C=N}$, imine); 1728 ($\nu_{C=O}$, ester); 3399 (ν_{OH}, H-bonded); ^{1}H NMR ($CDCl_3$, 300MHz): δ = 13.28 (bs, 2H, –OH); 8.69 and 8.61 (s, 2H, –CH=N); 8.16 (d, 4H, J = 8.8 Hz, ArH); 8.12 (d, 2H, J = 8.4 Hz, ArH); 7.43 (d, 1H, J = 8.2 Hz, ArH); 7.44 (d, 2H, J = 8.5 Hz, ArH); 7.12 (d, 1H, J = 2.5 Hz, ArH); 6.99 (d, 1H, J = 8.7 Hz, ArH); 6.94 (d, 2H, J = 2.6 Hz, ArH); 6.81 (d, 4H, J = 8.7 Hz, ArH); 4.08 (t, 4H, J = 6.2 Hz, –O–**CH_2**); 1.85 (q, 4H, J = 6.4 Hz, –CH_2–**CH_2**–); 1.56–1.24 (m, 60H, –**$(CH_2)_{15}$**); 0.86 (t, 6H, J = 6.6 Hz, –**CH_3**). Elemental analysis calculated for $C_{70}H_{95}O_8N_2F$ C = 75.64%; H = 8.61%; N = 2.52%. Found C = 75.67%; H = 8.63%; N = 2.55%.

3. Results and discussion

The starting material in the present study 4-(4-*n*-alkyloxybenzoyloxy)salicylaldehyde was prepared from 4-*n*-alkoxybenzoic acid by converting into acyl chloride followed by condensation with 2,4-dihydroxybenzaldehyde. The acyl group condensation with both of the hydroxyl groups in 2- and 4- positions is possible, condensation mainly takes place at the 4- position because of hydrogen bonding of the 2-hydroxyl group with the aldehyde oxygen and reaction conditions of the low temperature. The condensation 4-(4-*n*-alkyloxybenzoyloxy)salicylaldehyde with 4-fluoro-1,3-phenylenediamine in the presence of a few drops of glacial acetic acid yielded the target bent shaped compounds N,N′-bis[4-(4-*n*-alkyloxybenzoyloxy)salicylidene]-phenylene-4-fluoro-1,3-diamines, **3-*n*OHF** (n = 8, 10, 12 14, 16 and 18). To avoid the resulting side products under cold conditions in the solution, the precipitated compounds were filtered when the solution was hot to yield pure compounds and further recrystallised repeatedly. The formation of all of the compounds was confirmed by ^{1}H NMR and IR spectroscopy and the purity was established by elemental analysis. The liquid-crystalline behaviour of the synthesised compounds has been studied by optical microscopy and DSC.

3.1 Mesomorphic properties

The transition temperatures, enthalpies and entropies of the homologous series **3-*n*OHF** as a function of number of the carbon atoms in the terminal alkyl chains from DSC runs at a cooling rate of 10°C min^{-1} are presented in Table 1. The enthalpy changes corresponding to the clearing transition from mesophase to isotropic phase in banana compounds (**3-*n*OHF** series) are usually larger than those observed in calamitic compounds. The thermal data revealed that all of the compounds are exhibiting identical enantiotropic phase transitions except **3–8OHF**.

As shown in Figure 1, the clearing points increase moderately and the melting points decrease with the increasing chain length of the terminal alkoxy chains. All of the compounds exhibited liquid-crystalline behaviour with an identical texture as shown in Figure 2(a) observed for **3–14OHF**, characteristic of the $SmCP_A$ phase, which is further confirmed from the electro-optical and X-ray studies. Further cooling of the sample **3–14OHF** indicated another phase B_X, exhibiting a texture resembling the B4 phase which is yet to be confirmed (Figure 2(c)) (*15*). The $SmCP_A$ to B_X phase transformation is shown in Figure 2(b). The crystallisation from the B_X phase in general takes a longer duration of time, up to a few hours, and hence could not be detected. The supercooling effect of more than 15 K suggests that the B_X phase may be a B4 phase and further work by other experimental investigations, namely atomic force microscopy of thin films, optical studies of free-standing films, freeze fracture transmission electron microscopy and synchrotron X-ray studies are in progress to confirm the phase structure.

All of the homologues exhibited an identical texture indicating an unknown B_X phase, which is under further investigation. The homologue **3–8OHF** exhibits only a monotropic $SmCP_A$ phase. On cooling from the isotropic phase the circular domains appeared which are characteristic of $SmCP_A$ phase and the phase existence becomes broader for the longer chain homologues.

3.2 X-ray studies

In order to identify the model structure of the liquid-crystalline phases formed by these compounds, we conducted preliminary X-ray diffraction measurements on the **3–14OHF** homologue as a representative example using an image plate detector. Lindemann glass capillaries (1 mm diameter) were filled by a capillary action at high temperature without an alignment procedure to yield an unoriented sample and sealed under dry atmosphere. The capillary tube was introduced in an oven whose temperature stability was ±10 mK. The tube was vertical and perpendicular to the beam and the exposure times were maintained for 15 min. The X-ray diffraction experiments carried out on a non-oriented sample of the smectic phase of compound **3–14OHF** revealed the following features. In the small angle region one strong

Table 1. Transition temperatures (°C), enthalpies (italics kJ mol^{-1}) and entropies (italics in brackets J mol^{-1} K^{-1}) of homologous series **3-*n*OHF**.

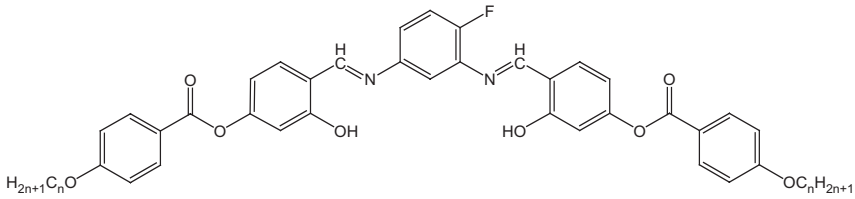

N, N′-bis[4-(4-n-alkyloxybenzoyloxy)salicylidene]phenylene-4-fluoro-1,3-diamines, **n = 8, 10, 12, 14, 16 and 18**

Compound	*R*	Cr	Heating cooling	B_X	Heating cooling	$SmCP_A$	Heating cooling	I
3–8OHF	C_8H_{17}	•			–	–	156.0	•
		•			141.4	•	[*40.3, 93.9*]	
					[*19.9, 48.2*]		149.2	
							[*14.6, 34.6*]	
3–10OHF	$C_{10}H_{21}$	•			147.6	•	159.0	•
					[*21.4, 51.0*]		[*17.2, 39.9*]	
		•		•	129.2	•	155.3	
					[*18.3, 45.5*]		[*14.4, 33.6*]	
3–12OHF	$C_{12}H_{25}$	•	109.5	•	142.5	•	162.9	•
			[*15.6, 40.9*]		[*23.3, 56.0*]		[*20.4, 46.8*]	
		•	108.9	•	121.3	•	158.6	
			[*1.4, 3.8*]		[*19.9, 50.5*]		[*18.8, 45.4*]	
3–14OHF[a]	$C_{14}H_{29}$	•	111.3	•	138.1	•	163.0	•
			[*12.4, 32.2*]		[*22.9, 55.8*]		[*19.9, 45.8*]	
		•	109.1		114.0	•	158.2	
			[*15.9, 41.9*]		[*17.4, 45.1*]		[*17.0, 39.4*]	
3–16OHF[b]	$C_{16}H_{33}$	•	114.8	•	134.0	•	162.8	•
			[4.4, *11.4*]		[*15.1, 37.1*]		[*8.12, 18.6*]	
		•	109.4	•	113.6	•	160.3	
			[*2.56, 6.7*]		[*8.54, 22.0*]		[*10.2, 23.6*]	
3–18OHF[c]	$C_{18}H_{37}$	•	119.5	•	134.9	•	162.4	•
			[*38.6, 98.4*]		[*18.5, 45.3*]		[*19.3, 44.3*]	
		•	112.8	•	115.4	•	159.6	
			[*5.0, 12.9*]		[*1.8, 4.6*]		[*20.1, 46.5*]	

All of the reported temperatures are the peak recorded in DSC thermographs in the first heating and cooling cycles at heating and cooling rates of 10°C min^{-1}. Additional crystal-to-crystal transitions have been observed in the heating cycle **3–14OHF** ([a]100.4 [*5.6, 15.0*]); ([b]106.1 [*14.8, 39.1*]) and in the cooling cycle ([c]103.8 [*4.3, 11.3*]).

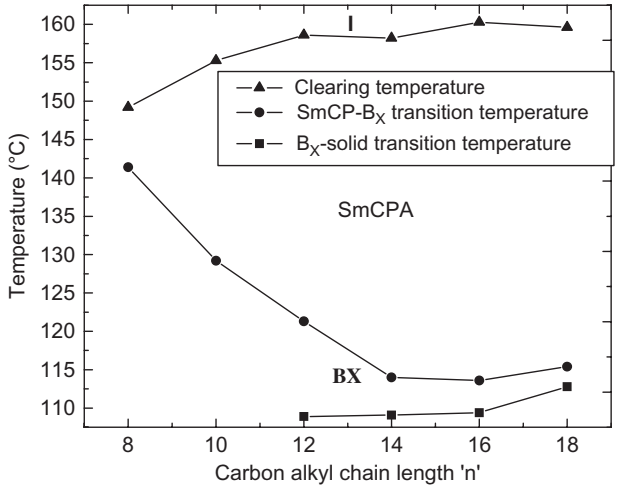

Figure 1. Phase diagram of the Bis-[4-(4′-n-alkyloxy benzoyloxy)-salicylidene]-phenylene-4-fluoro-1,3-diamines in cooling cycle.

reflection (Figure 2(d)) was observed at d = 4.10 nm revealing the layer structure.

The value for the first reflection is considerably smaller than the length of the molecule **(3–14OHF)** (L = 6.33 nm) as measured along the 'bow axis' (also the director direction for the bent-core molecules) by assuming that the methylene chains are fully extended in the all-trans conformation (Figure 3) and the tilt angle (θ) of the molecules was estimated to be 49° which is little larger than the optical tilt angle (~46°) observed between the extinction brushes in the electro-optical measurements during the switching process. Such large tilt angles up to 56° are reported in literature in lateral fluoro substituted compounds exhibiting $SmCP_A$ phases (*7*). Further broad diffuse scattering maxima in the wide-angle region around 0.47 nm indicated a liquid like in-plane order with no long-range positional order within the smectic layers. Further during the transition from $SmCP_A$ to a

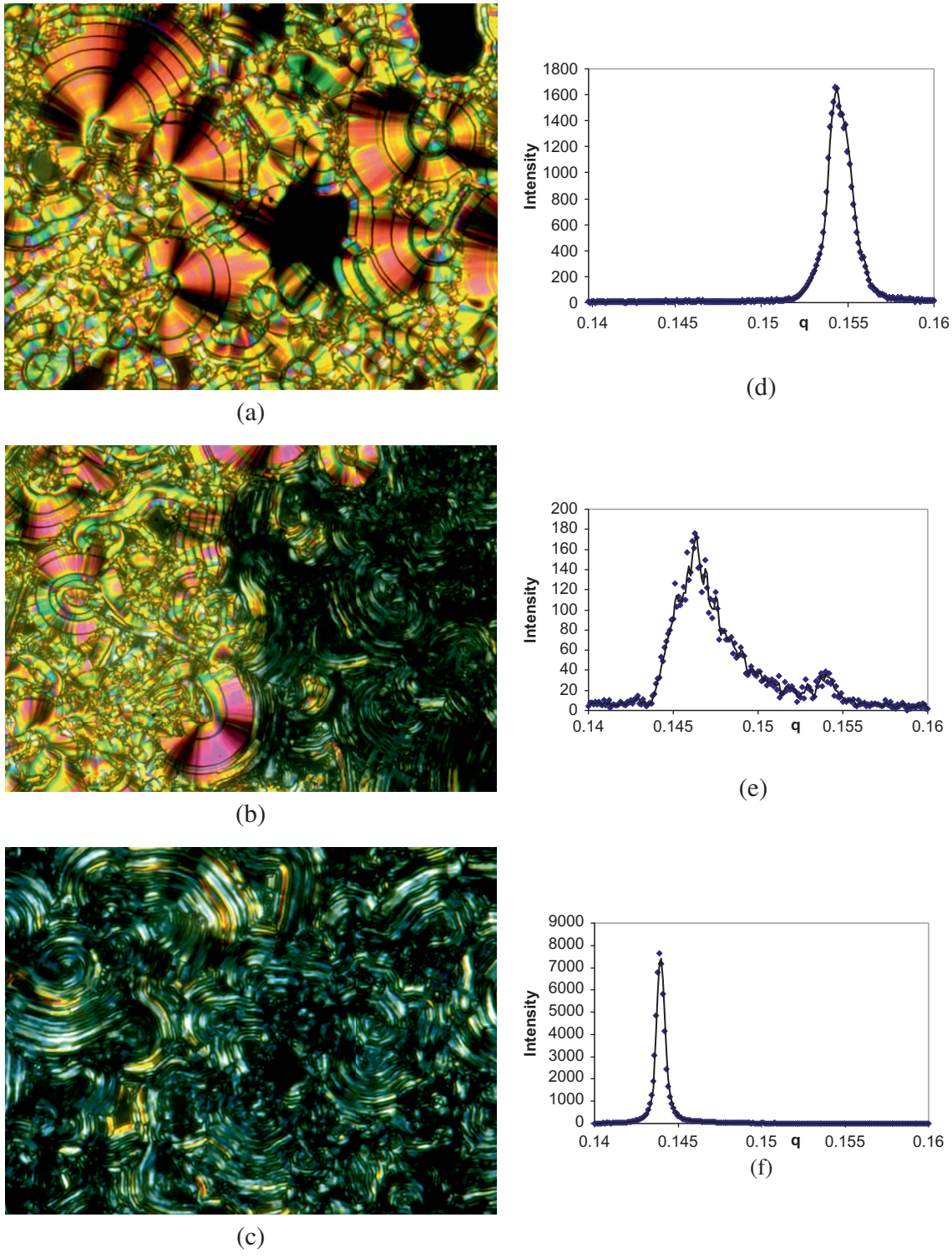

Figure 2. Characteristic textures exhibited by **3–14OHF** and intensity profiles of X-ray diffraction patterns. (a) $T = 158.0°C$. (b) During the transition at $T = 114.0°C$. (c) Smectic B_X phase below the phase transition at 113.2°C. (d) Intensity profile of the X-ray diffraction pattern in the small angle region at $T = 154°C$. (e) Intensity profile of the X-ray diffraction pattern in the small angle region during the transition at $T = 114°C$. (f) Intensity profile of the X-ray diffraction pattern in the small angle region at $T = 92°C$.

low-temperature phase, with the disappearance of the existing peak and appearance of the strong reflection indicating another smectic phase with an increase in layer thickness (Figure 2(e), 4.30 nm). On further cooling the peak grows stronger (Figure 2(f)) and continued until room temperature.

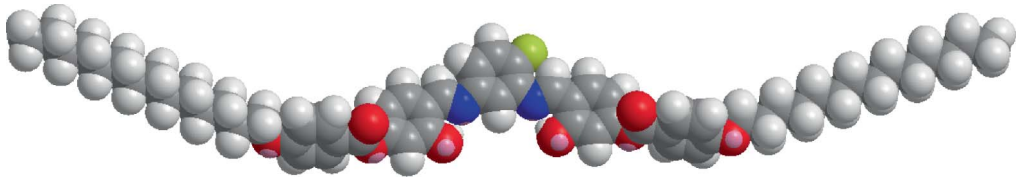

Figure 3. Molecular model of compound **3–14OHF** in which the chains are in a fully extended all-trans conformation.

3.3 Electro-optical investigations

The mesophase exhibited by compounds **3-*n*OHF** shows electro-optical switching behaviour. The switching behaviour of the SmCPA phase was observed using electro-optical measurements as well as simultaneous observation of changes in the thin films of the compound under a polarising microscope. The sample was filled in a freshly assembled 5 μm polyimide-coated homogenous cell in the isotropic phase and cooled slowly into the mesophase at a rate of 0.5°C min^{-1}. After the sample is cooled into the mesophase 5°C below the mesophase–isotropic phase transition temperature, the applied field is gradually increased to obtain aligned samples and saturated current peaks. The application of a sufficiently large triangular voltage yielded the current response peaks in each half period of the waveform. The current response of compound **3–14OHF** (see Figure 4) shows two polarisation current peaks for each half cycle on applying a triangular-wave electric field of about ±80 V, 50 Hz, at 145°C, indicating an antiferroelectric ground state structure in the mesophase, and the spontaneous polarisation was found to be ~528 nC cm^{-2}, which is comparable with the reported values in the $SmCP_A$ phase of compounds possessing a lateral dipole moment. The variation of spontaneous polarisation, which is found to be temperature dependent, is shown in Figure 5. The electro-optical behaviour response of this sample was observed as textural changes by the application of an electric field.

The influence of a d.c. electric field on the molecular alignment, which is reflected in the optical textures of compound **3–14OHF** filled in readymade unidirectional polyimide-coated 5 μm thin commercial cells purchased from Instec Inc., is as follows. On cooling the isotropic phase of the compound **3–14OHF** in the absence of an electric field, it transformed into a SmCP-type liquid-crystalline phase at 158.2°C with the appearance of a characteristic striped texture with spherulitic growth (Figure 6(a)) and tends to grow fan-shaped domains (with horizontal and vertical Maltese crosses making an angle with the polariser) with a fringe pattern showing helical structure.

The majority of the domains exhibited a striped pattern texture with equal spacing of the stripes. This texture is reminiscent of the 'fingerprint' texture expected for helical banana phase structures, with the molecular plane parallel to the cell surface and the tilted smectic layers, with a tilt equal to the director tilt angle, aligned perpendicular to the plane of the cell surface (bookshelf geometry). (The director is along

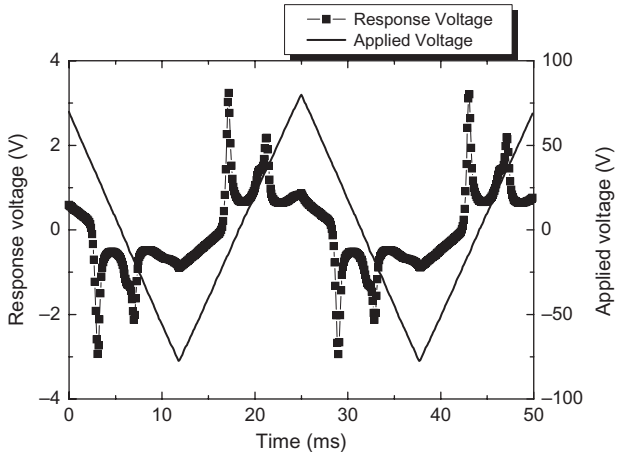

Figure 4. Switching current response obtained for the compound **3–14OHF** by applying a triangular wave electric field at (±80 $V_{pp,}$ 50 Hz) at T = 145°C. Sample thickness 5 μm; spontaneous polarisation, P_S ~ 528 nC cm^{-2}.

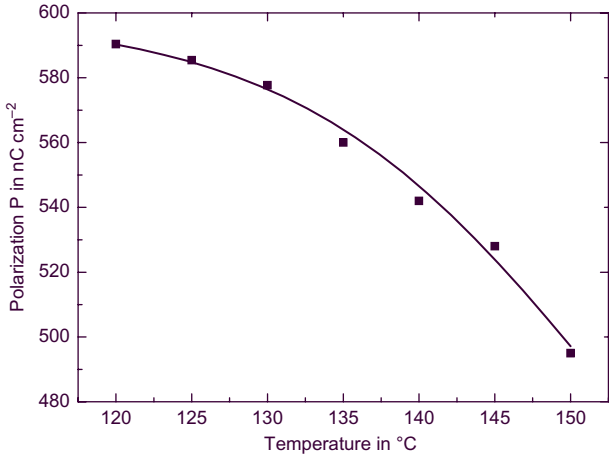

Figure 5. Temperature variation of spontaneous polarisation in the $SmCP_A$ phase of compound **3–14OHF**.

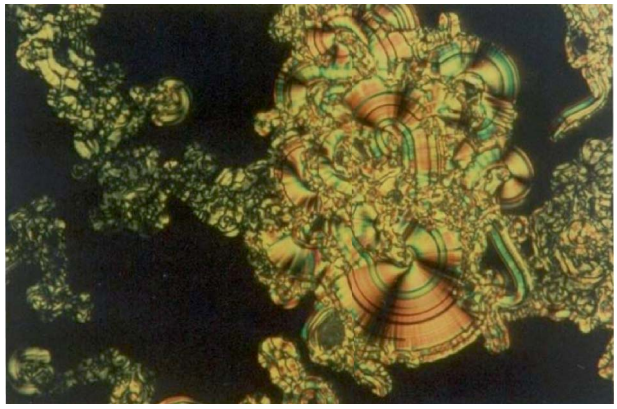

(a)

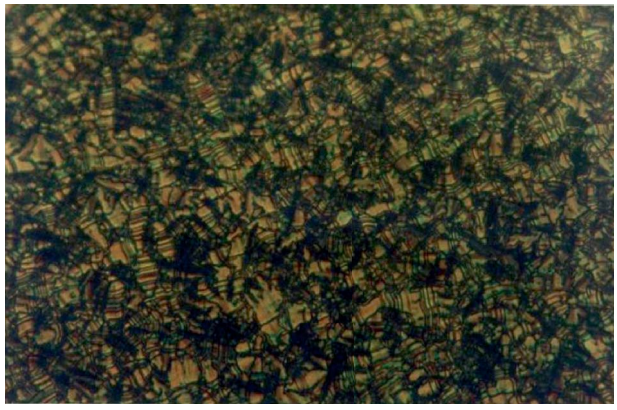

(b)

(c)

Figure 6. Optical texture of the $SmCP_A$ phase of compound **3–14OHF** under the influence of an electric field: spherulitic growth with coloured stripes. Thickness of cell = 5 μm. (a) Without an electric field. (b) Electric field = 6 V μm^{-1}, T = 154°C. (c) Optical texture of the $SmCP_A$ phase of the compound **3–14OHF** cooled from the isotropic phase under the influence of an electric field of 10 V and after the removal of the field, T = 154°C.

the layer normal and the molecules can have either a synclinic or an anticlinic interlayer correlation.) Consistent with the helical structure, it is apparent that the stripes are oriented parallel to the layers in the focal conic texture. It is apparent from the equally spaced striped lines that the layers are flat and parallel to each other and the curved complex patterns on the macroscopic length support the formation of the random focal conic fan texture. The switching behaviour of the $SmCP_A$ phase of the compound **3–14OHF** under a d.c. electric field has been examined using a polarising microscope. On cooling from the isotropic phase the sample under the influence of an electric field of ±6 V μm^{-1} exhibiting an equally spaced striped texture (Figure 6(b)), with a spherulitic growth in the entire region with homeotropic regions. A further increase in the strength of the electric field ±10 V μm^{-1} leads to the appearance of stable colourful stripes with a change in birefringence of the texture. The sample is cooled under the influence of a field (±10 V μm^{-1}) and when the field is switched off the texture (as shown in Figure 6(c)) becomes non-birefringent with more dark regions. These preliminary studies of optical textures confirm the identification of the mesophase as a $SmCP_A$ phase which is similar to the fringe texture of the $SmCP_A$ mesophase of PIMB series (*16*). The detailed electro-optic measurements are in progress and the results will be reported elsewhere.

3.4 Structure–property relationship

3.4.1 Influence of the functional group

The molecular structures of different compounds **A–D** of five-membered ring molecular bent-core skeletons with a change in the substituent are depicted in Figure 7. The liquid-crystal properties and phase transition temperatures were greatly affected by the subtle changes in chemical structure. In the unsubstituted homologous series, namely N,N′-bis[4-(4′-*n*-alkyloxybenzoyloxy)benzylidene]-phenylene-1,3-diamines (compound **A, 3-*n*HH** without fluoro and ortho hydroxyl substituent analogues) lower homologues (with carbon chain length n = 1–4) exhibited a B6 phase, while middle homologues (n = 7–10) exhibited B6 and B1 phases. However, the higher homologues with n = 11 and 12 exhibited a monotropic B2 phase as transient phenomena for a shorter duration which did not allow any experimental studies (*17*).

In order to make a comparison with the compounds reported here we synthesised two additional compounds possessing an ortho hydroxyl group **(B)** or 4- fluoro group **(C)**. The compounds N,N′-bis[4-(4′-*n*-decyloxybenzoyloxy)salicylidene]-phenylene-1,3-diamine (**3–10OHH, B**) and N,N′-bis[4-(4′-*n*-decyloxybenzoyloxy)benzylidene]-phenylene-4-fluoro-1,3-diamine (**3–10HF, C**) are studied for their mesomorphism by thermal microscopy and DSC. The compound **B** exhibited an unspecific grainy texture with

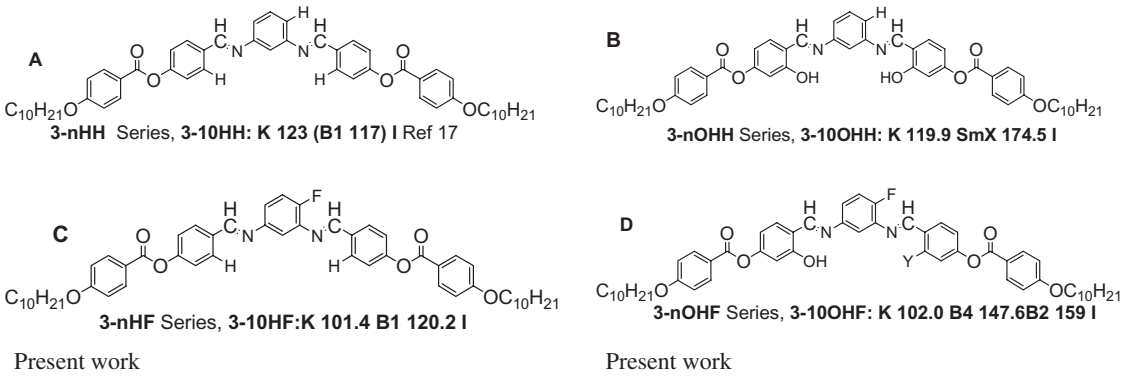

Figure 7. Five-membered ring molecular bent-core skeleton with a change in substituent.

enantiotropic phase transitions with higher thermal stability. The compound **C** exhibited a texture (as shown in Figure 8) resembling the B1 phase observed in other compounds reported in the literature (*5*, *6*). The introduction of a fluoro substituent at a lateral position of the central phenyl ring, compound **C,** not only changes the nature of mesomorphism from monotropic to enantiotropic phase behaviour, but also causes a moderate reduction in clearing temperatures when compared with the unsubstituted compounds **A** and **B**. The introduction of a fluoro group in the central core in addition to the ortho hydroxyl group stabilising the imine linkage in the lateral ring by intermolecular or intramolecular hydrogen bonding which resists hydrolysis (in the compounds reported in this paper) completely changed the mesophase behaviour of these compounds, **D**, to exhibit $SmCP_A$ and B_X phases as compared with the B6, B1, B2 phases exhibited by unsubstituted compounds **A** and **B**.

3.4.2 Influence of the linkage group

However, when the imine linkage at the central core is reversed the resulting unsubstituted homologues of 1,3-phenylene-bis-[4-(4′-alkoxybenzoyloxy)-phenyliminomethane] family (**C*n*** series) also exhibited B1 (C5–C9 lower homologues) and $SmCP_A$ (C10–C14 higher homologues) phases (*18*). The C12 homologue **E** (Figure 9) exhibits a $SmCP_A$ phase and spontaneous polarisation is of the order of 350 nC cm^{-2}, which is smaller than the $P_S \sim 590$ nC cm^{-2} found in the present investigation. However, if the ester linkage and salicylideneimine linkage are swapped (*19*), then the resulting materials **F** (BCH) without a fluoro group in the central core also exhibited switchable B2 or B1 ($P_S \sim$ 500 nC cm^{-2} for a C10 homologue (*19b*)) or B7 (C16 homologue) phases depending on the end alkyl chain length, which indicates the importance of the ortho hydroxyl group and the position of linking groups. The homologues with chloro or nitro substituents in the central core exhibited a $SmCP_A$ phase.

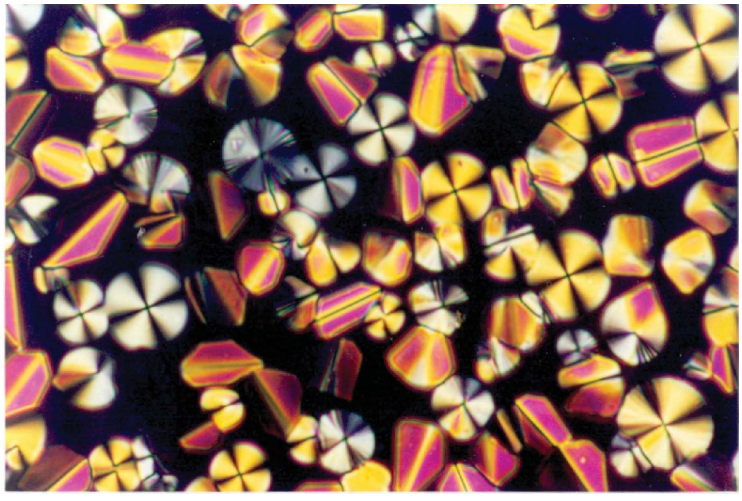

Figure 8. Optical texture of the B1 phase of the compound **3–10HF**.

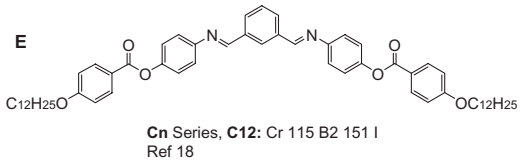

Cn Series, **C12:** Cr 115 B2 151 I
Ref 18

Linking group is reversed

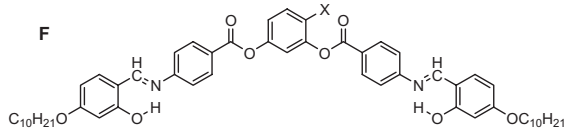

C10-homologue: BC-H X =H, Cr 117.0°C $SmCP_A$ 178.5°C, Ps ~ 500 nC.cm^{-2}
C11-homologue: BC-Cl X = Cl, Cr 110.5°C $SmCP_A$ 151.5°C; Ps =129nC.cm^{-2}
C7-homologue: BC-NO_2 X = NO_2, Cr 104.9°C $SmCP_A$ 178.8°C Ps = 484 nC.cm^{-2}
Ref. 19

Swapping of linking groups

Figure 9. Bent-core molecular skeleton with reversed imine linkage **E,** or swapped imine and ester linkages **F**.

3.4.3 Influence of fluorine in the outermost ring

With the introduction of fluoro substitution into the outermost rings instead of the central ring, the homologues of 1,3-phenylene-bis[4-(4′-alkoxybenzoyloxy)-phenyliminomethane] family (**D*n*F** series, **G, H** and **I**; Figure 10) exhibited different types of banana phases depending on the position of substitution with an increase or decrease in transition temperatures (*20*). The compound **G** with a fluoro atom in the ortho position to the ester linkage exhibited a $SmCP_A$ phase. However, when the fluoro atom is in a meta position with respect to ester linkage, the compound **H** exhibited a ferroelectric $SmB7_{bis}$ phase with P_S value varying between 300 and 380 nC cm^{-2}. The compound **F** with two fluoro atoms exhibited a ferroelectric phase which over time relaxed to an antiferroelectric phase.

DnF2 Series, **D14F2:** Cr97 $SmCP_A$ 131.0 I
Ref. 20

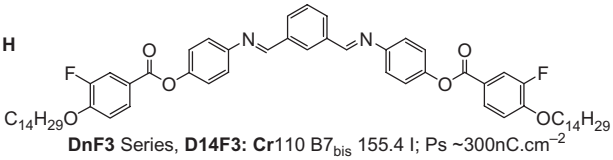

DnF3 Series, **D14F3: Cr**110 $B7_{bis}$ 155.4 I; Ps ~300nC.cm^{-2}
Ref. 20

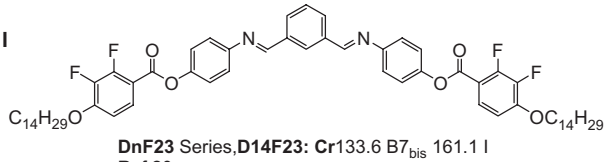

DnF23 Series,**D14F23: Cr**133.6 $B7_{bis}$ 161.1 I
Ref 20

Figure 10. Bent-core molecular skeleton with fluoro substituent in the wings.

4. Conclusions

The reported observation (*21*) regarding the influence of the fluoro atom in the 4- position of the central core, a derivative of isophthalic acid that does not modify the mesomorphic domain and the phase sequence in comparison with the compounds without a substituent, is always not true. The nature of the substituent, combination and the direction of different linking groups in each arm of the bent shaped molecule, the position of the substituent either on the central core or other rings of the molecule and the length of aliphatic end chains collectively play a very important role in deciding the nature of banana mesophases. In the present homologous series, the hydrogen bonding may be intramolecular or intermolecular and the combination of a specific substituent such as a fluorine atom replacing the H atom in the central core not only enhances the polarisability due to its large dipole moment, but also has a major influence on the mesophase behaviour leading to banana mesomorphism.

Acknowledgements

Financial support was provided by DST, DAE and DRDO. We are grateful to Professor K. A. Suresh, Professor N. A. Clark and Dr C. Jones for their help in providing some experimental facility.

References

(1) Niori, T.; Sekine, T.; Watanabe, J.; Furukawa, T.; Takezoe, H. *J. Mater. Chem.* **1996**, *6*, 1231–1233.
(2) Pelzl, G.; Diele, S.; Weissflog, W. *Adv. Mat.* **1999**, *11*, 707–724.
(3) (a) Link, D.R.; Natale, G.; Shao, R.; Maclennan, J.E.; Clark, N.A.; Korblova, E.; Walba, D.M. *Science* **1997**, *278*, 1924–1927. (b) Walba, D.M.; Korblova, E.; Shao, R.; Maclennan, J.E.; Link, D.R.; Glaser, M.A.; Clark, N.A. *Science* **2000,** *288*, 2181–2184. (c) Heppke, G.; Moro, G. *Science* **1998,** *27*, 1872–1873.
(4) Ros, M.B.; Serrano, J.L.; de la Fuente, M.R.; Folcia, C.L. *J. Mater. Chem.* **2005**, *15*, 5093–5098.
(5) Reddy, B.A.; Tschierske, C. *J. Mater. Chem.* **2006**, *16*, 907–961.

(6) Takezoe, H.; Takanishi, Y. *Jpn. J. Appl. Phys.* **2006**, *45*, 597–625

(7) (a) Weissflog, W.; Nadasi, H.; Dunemann, U.; Pelzl, G.; Diele, S.; Eremin, A.; Kresse, H. *J. Mater. Chem.* **2001**, *11*, 2748–2758. (b) Pelzl, G.; Diele, S.; Grande, S.; Jakli, A.; Lischka, C.; Kresse, H.; Schmalfuss, H.; Wirth, I.; Weissflog, W. *Liq. Cryst.* **1999,** *26*, 401–413. (c) Wirth, I.; Diele, S.; Eremin, A.; Pelzl, G.; Grande, S.; Kovalenko, L.; Pancenko, N.; Weissflog, W. *J. Mater. Chem.* **2001,** *11*, 1642–1650. (d) Shubashree, S.; Sadashiva, B.K.; Dhara, S. *Liq. Cryst*. **2002,** *29*, 789–797.

(8) (a) Dunemann, U.; Schroder, M.W.; Reddy, R.A.; Pelzl, G.; Diele, S.; Weissflog, W. *J. Mater. Chem.* **2005**, *15*, 4051–4061. (b) Dantlgraber, G.; Shen, D.; Diele, S.; Tschierske, C. *Chem. Mater.* **2002,** *14*, 1149–1158. (c) Shen, D.; Pegenau, A.; Diele, S.; Wirth, I.; Tschierske, C. *J. Am. Chem. Soc*. **2000,** *122*, 1593–1601. (d) Shen, D.; Diele, S.; Pelz, G.; Wirth, I.; Tschierske, C. *J. Mater. Chem.* **1999,** *9*, 661–672. (e) Shen, D.; Diele, S.; Wirth, I.; Tschierske, C. *Chem. Commun.* **1998,** 2573–2574.

(9) (a) Weissflog, W.; Kovalenko, L.; Wirth, I.; Diele, S.; Pelzl, G.; Schmalfuss, H.; Kresse, H. *Liq. Cryst.* **2000**, *27*, 677–681. (b) Nguyen, H.T.; Rouillon, J.C.; Marcerou, J.P.; Bedel, J.P.; Barois, P.; Sarmento, S. *Mol. Cryst. Liq. Cryst.*, **1999,** *328*, 177–184.

(10) (a) Weissflog, W.; Lischka, Ch.; Benne, I.; Scharf, T.; Pelzl, G.; Diele, S.; Kruth, H. *Proc. SPIE*, **1998**, *3319*, 14–19. (b) Pelzl, G.; Schroder, M.W.; Dunemann, U.; Diele, S.; Weissflog, W.; Jones, C.; Coleman, D.; Clark, N.A.; Stannarius, R.; Li, J.; Das, B.; Grande, S. *J. Mater. Chem.* **2004,** *14*, 2492–2498.

(11) (a) Nadasi, H.; Weissflog, W.; Eremin, A.; Pelzl, G.; Diele, S.; Das, B.; Grande, S. *J. Mater. Chem.*, **2002**, *12*, 1316–1324. (b) Reddy, R.A.; Sadashiva, B.K. *J. Mater. Chem.* **2004,** *14*, 1936–1947. (c) Murthy, H.N.S.; Sadashiva, B.K. *J. Mater. Chem.* **2004,** *14*, 2813–2821. (d) Yelamaggad, C.V.; Shashikala, I.S.; Hiremath, U.S.; Liao, G.; Jakli, A.; Rao, D.S.S.; Prasad, S.K.; Li, Q. *Soft Matter* **2006,** *2*,785–792.

(12) (a) Smart, B.E. In *Organofluorine Chemistry Principles and Commercial Applications*, Banks, R.E., Smart, B.E. and Tatlow, J.C., Eds.; Plenum Press: New York, 1994, p. 57. (b) Guittard, F.; Geribaldi, S. *J. Fluorine Chem.* **2001,** *107*, 363–374. (c) Guittard, F.; deGivenchy, E.T.; Geribaldi, S.; Cambon, A. *J. Fluorine Chem.* **1999,** *100*, 85–96. (d) Hunter, C.A.; Sanders, J.K.M. *J. Am. Chem. Soc*. **1990,** *112*, 5525–5534.

(13) (a) Thisayukta, J.; Nakayama, Y.; Kawauchi, S.; Takezoe, H.; Watanabe, J. *J. Am. Chem. Soc.* **2000**, *122*, 7441–7448. (b) Araoka, F.; Park, B.; Kinoshita, Y.; Takezoe, H.; Thisayukta, J.; Watanabe, J. *Mol. Cryst. Liq. Cryst.* **1999,** *328*, 291–297. (c) Nakata, M.; Link, D.R.; Thisayukta, J.; Takanishi, Y.; Ishikawa, K.; Watanabe, J.; Takezoe, H. *J. Mater. Chem.* **2001,** *11*, 2694–2699. (d) MacDonald, R.; Kentischer, F.; Warnick, P.; Heppke, G. *Mol. Cryst. Liq. Cryst.* **1999,** *320*, 101–108.

(14) (a) Ghedini, M.; Panuzi, B.; Roviello, A. *Liq. Cryst.* **1998**, *25*, 225–233. (b) Hoshino, N.; Kodama, A.; Shibuya, T.; Matsunaga, Y.; Miyajima, S. *Inorg. Chem.* **1991,** *30*, 3091–3096.

(15) (a) Watanabe, J.; Niori, T.; Sekine, T.; Takezoe, H. *Jpn. J. Appl. Phys.* **1998**, *37*, L139–L142. (b) Sekine, T.; Niori, T.; Sone, M.; Watanabe, J.; Choi, S.W.; Takanishi, Y.; Takezoe, H. *Jpn. J. Appl. Phys.* **1997,** *36*, 6455–6463. (c) Thisayukta, J.; Niwano, H.; Takezoe, H.; Watanabe, J. *J. Mater. Chem.* **2001,** *11*, 2717–2721. (d) Thisayukta, J.; Nakayama, Y.; Kawauchi, S.; Takezoe, H.; Watanabe, J. *Jpn. J. Appl. Phys.* **2001,** *40*, 3277–3287.

(16) Nadasi, H.; Lischka, Ch.; Weissflog, W.; Wirth, I.; Diele, S.; Pelzl, G.; Kresse, H. *Mol. Cryst. Liq. Cryst.* **2003**, *399*, 69–84.

(17) Weissflog, W.; Wirth, I.; Diele, S.; Pelzl, G.; Schmalfuss, H.; Schoss, T.; Wurflinger, A. *Liq. Cryst.* **2001**, *28*, 1603–1609.

(18) Bedel, J.P.; Rouillon, J.C.; Marcerou, J.P.; Laguerre, M.; Achard, M.F.; Nguyen, H.T. *Liq. Cryst.* **2000**, *27*, 103–113.

(19) (a) Walba, D.M.; Korblova, E.; Shao, R.; Clark, N.A. *J. Mater. Chem.* **2001**, *11*, 2743–2747. (b) Yelamaggad, C.V.; Hiremath, U.S.; Nagamani, S.A.; Rao, D.S.S.; Prasad, S.K. *J. Mater. Chem.* **2001,** *11*, 1818–1822. (c) Rao, D.S.S.; Nair, G.G.; Prasad, S.K.; Nagamani, S.A.; Yelamaggad, C.V. *Liq. Cryst.* **2001,** *28*, 1239–1243. (d) Prasad, S.K.; Maeda, Y.; Rao, D.S.S.; Nagamani, S.A.; Hiremath, U.S.; Yelamaggad, C.V. *Liq. Cryst.* **2003,** *30*, 1277–1283. (e) Yelamaggad, C.V.; Mathews, M.; Nagamani, S.A.; Rao, D.S.S.; Prasad, S.K.; Findeisen, S.; Weissflog, W. *J. Mater. Chem.* **2007,** *17*, 284–298. (f) Achten, R.; Koudijs, A.; Karczmarzyk, Z.; Marcelis, A.T.M.; Sudholter, E.J.R. *Liq. Cryst.* **2004,** *31*, 215–227.

(20) Bedel, J.P.; Rouillon, J.C.; Marcerou, J.P.; Laguerre, M.; Nguyen, H.T.; Achard, M.F. *J. Mat. Chem.* **2002**, *12*, 2214–2220.

(21) Nguyen, H.T.; Bedel, J.P.; Rouillon, J.C.; Marcerou, J.P.; Achard, M.F. *Pramana* **2003**, *61*, 395–404.